DSP-Based Nonlinear SNR Estimation via Longitudinal Power Monitoring in Commercial Coherent Receivers

DSP-Based Nonlinear SNR Estimation via Longitudinal Power Monitoring in Commercial Coherent Receivers

Gabriella Bosco
DET, Politecnico di Torino
Torino, Italy
gabriella.bosco@polito.it

Lorenzo Andrenacci
DET, Politecnico di Torino
Torino, Italy
lorenzo.andrenacci@polito.it

Antonino Nespola
Links Foundation
Torino, Italy
antonino.nespola@linksfoundation.com

Stefano Straullu
Links Foundation
Torino, Italy
stefano.straullu@linksfoundation.com

Yanchao Jiang
DET, Politecnico di Torino
Torino, Italy
yanchao.jiang@polito.it

Stefano Piciaccia
Cisco Photonics Italy S.r.l.
Vimercate, Italy
spiciacc@cisco.com

Dario Pilori
DET, Politecnico di Torino
Torino, Italy
dario.pilori@polito.it

***Abstract*—The signal-to-noise ratio (SNR) measured on the received symbol constellation, accounting for both amplified spontaneous emission (ASE) noise and Kerr-induced nonlinear interference (NLI), is a key metric for system design and optimization. Consequently, separating these noise contributions enables the optimization of optical networks for more efficient and lower-margin transmissions. However, recent methods for nonlinear SNR estimation, such as artificial neural networks and statistical noise manipulation, require extensive knowledge of transmission parameters or large training datasets. In this work, an alternative approach, which requires minimal information about the system configuration, is described and validated through simulations and experiments. It exploits a linear least squares (LLS)-based longitudinal power monitoring (LPM) algorithm that can be implemented in standard coherent receivers, combined with analytical expressions based on closed-form NLI models (e.g., the GN model). In addition, the practical implementation challenges of using hard-decided symbols to generate reference signals for LLS-based LPM in NLI estimation are explored.**

***Index Terms*—Optical Performance Monitoring, Longitudinal Power Monitoring, Nonlinear Penalty Estimation.**

I. Introduction

THE increasing demand for higher capacity and greater flexibility in modern optical communication networks presents significant challenges for network operation and management. As traffic patterns become more dynamic, the ability to adjust optical paths and switch wavelengths efficiently is essential. Additionally, low-margin operation and optimal allocation of network resources are key concerns for network designers. To address these challenges, telemetry data obtained from coherent transceivers plays a critical role in network monitoring and optimization.

Coherent transceivers already provide valuable telemetry information through their digital signal processing (DSP) modules [1]. Among the available telemetry metrics, the constellation signal-to-noise ratio (SNR) is particularly important, since it directly determines bit error ratio (BER) and generalized mutual information (GMI) [2]. After propagation over a coherent optical link, the SNR (in linear units) can be expressed as [3]:

$$\mathrm{SNR} = (\mathrm{SNR}_{\mathrm{TRX}}^{-1} + \mathrm{OSNR}^{-1} + \mathrm{SNR}_{\mathrm{NL}}^{-1})^{-1} \tag{1}$$

where $\mathrm{SNR}_{\mathrm{TRX}}$ accounts for transceiver noise, OSNR for ASE noise and $\mathrm{SNR}_{\mathrm{NL}}$ for Kerr-induced NLI; the OSNR is computed on a reference bandwidth equal to the symbol rate. Isolating the above three noise components is essential for network optimization, as the optimal optical transmit power per span depends on the relative power of ASE and NLI noise [3]. While transceiver noise can be characterized via factory calibration, separating ASE and NLI contributions remains challenging.

Various methods have been proposed to separate NLI power. Some methods leverage the non-Gaussian nature of NLI [4] to extract its power from carrier phase recovery (CPR) algorithms or time-domain correlations in received constellation diagrams [5]–[7]. However, these techniques require ideal conditions and prior link knowledge. Others methods introduce frequency-domain notches to facilitate noise separation [8], needing transmitter modifications and calibration. Machine learning approaches analyze constellation distortions [9]–[11] or SNR fluctuations [12] but lack physical interpretability and require extensive training.

Recently, digital longitudinal monitoring (DLM) has emerged as a promising alternative, using receiver DSP data for power profile and link parameter estimation [13], [14]. DLM has been successfully applied to estimate power profiles, CD maps, amplifier gain spectra, optical filters' impulse responses [15] and PDL [16]. A major advantage of DLM is that it relies solely on information already available in receiver DSP, making it well-suited for integration into coher-

979-8-3315-9777-1/25/$31.00 ©2025 IEEE

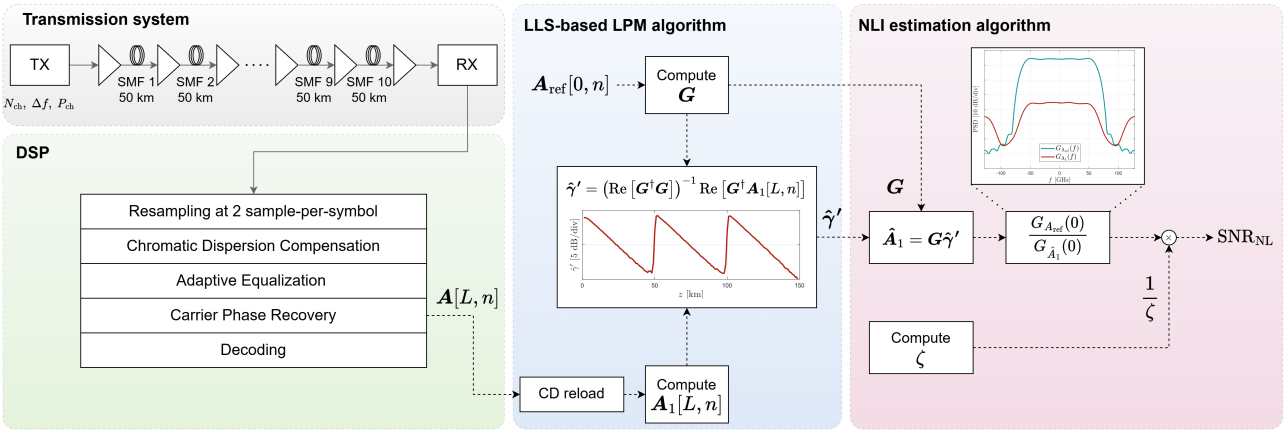

Fig. 1. Schematic of the simulation setup and DSP used to validate the proposed method.

ent transceivers [17]. One specific DLM method, LLS-based longitudinal power monitoring (LPM) [18], can accurately track optical power evolution. When combined with simplified NLI models like the GN model [3], LPM enables precise NLI estimation. By combining NLI estimates with transceiver calibration data and overall SNR measurements, the three noise components—transceiver noise, ASE noise, and NLI—can be effectively segregated.

A preliminary suggestion for this type of solution was presented in [15], with one implementation proposing the use of estimated power profiles for split-step Fourier method (SSFM) simulations to determine NLI power [19]. However, this approach is computationally demanding, as it requires re-propagation of all WDM channels, which are generally unavailable at the receiver. Another potential method involves using LPM to estimate link parameters necessary for analytical NLI models (e.g., GN or EGN models). While viable, this is an indirect estimation approach, meaning that inaccuracies in link parameters can propagate into the NLI model, degrading performance. In [20], [21] a more direct approach was proposed, demonstrating how NLI estimation is inherently integrated within LLS-based LPM. This method was validated across a wide range of simulations and experimental conditions.

While LLS-based LPM requires limited receiver DSP data to compute the power profile (specifically the received – noisy – constellation symbols and their corresponding noise-free transmit symbols [18]), obtaining noise-free transmit symbols in real-time receivers is nontrivial. In [17] the authors showed that substituting the transmit sequence with hard-decision (HD) estimates of the received constellation introduces only a small offset in the power profile, which can be compensated for. The practical effects of power estimation offsets on NLI determination using LLS-based LPM were investigated in [22] validating the results in an experimental transmission over a 17×65 km standard single-mode fiber (SSMF) link. The obtained results demonstrate that this novel approach effectively isolates NLI without requiring extensive prior calibration or transmitter modifications, making it a promising candidate for practical network monitoring and optimization.

In this paper, we review the latest proposed solutions for NLI estimation through LLS-based LPM, also addressing the practical implementation challenge of the use of hard-decision symbols for the generation of the reference signals required by the algorithm

II. NLI Estimation from Linear Least Squares-based LPM

The NLI estimation algorithm discussed in this work, and schematically depicted in Fig. 1, was proposed in [21] and resorts to LLS-based LPM [18]. It consists in estimating the power profile evolution $\gamma' = \frac{8}{9}\gamma\mathbf{P}$ of a WDM optical signal $\mathbf{A}$ in the propagation direction and using it to reconstruct its first-order nonlinear approximation term $\mathbf{A}_1$. This term carries information on NLI and can be expressed in matrix form as $\mathbf{A}_1 \simeq \mathbf{G}\gamma'$, where $\mathbf{G}$ is a perturbation matrix computed from a reference version of the transmitted signal $\mathbf{A}_{\text{ref}}$ [18].

The nonlinear SNR can then be computed as:

$$\text{SNR}_{\text{NL}} = \frac{1}{\zeta}\frac{G_{\mathbf{A}_{\text{ref}}}}{G_{\mathbf{A}_1}} \tag{2}$$

where $G_{\mathbf{A}_{\text{ref}}}$ and $G_{\mathbf{A}_1}$ are the power spectral densities (PSDs) of $\mathbf{A}_{\text{ref}}$ and $\mathbf{A}_1$, here assumed flat over the channel bandwidth. The factor ζ, instead, is a correction term introduced to account for the cross-channel interference (XCI) contribution to NLI, since LPM includes only self-channel interference (SCI):

$$P_{\text{NLI}} \approx P_{\text{SCI}} + P_{\text{XCI}} = P_{\text{SCI}}\left(1 + \frac{P_{\text{XCI}}}{P_{\text{SCI}}}\right) = P_{\text{SCI}} \cdot \zeta \tag{3}$$

If all the parameters of the link are known, ζ can be easily obtained by using any NLI model. For instance, if we consider as COI the central channel of a homogeneous WDM comb, comprising N_{ch} channels with a symbol rate R_{s} and spaced by Δf, we can apply the straightforward closed-form approximation provided by the GN model [23, Eq. (15)], yielding

$$\zeta \approx \frac{\operatorname{asinh}\left(\frac{\pi^2}{2}\beta_2 L_{\text{eff,a}} R_{\text{s}}^2 N_{\text{ch}}^{\frac{2R_{\text{s}}}{\Delta f}}\right)}{\operatorname{asinh}\left(\frac{\pi^2}{2}\beta_2 L_{\text{eff,a}} R_{\text{s}}^2\right)}. \tag{4}$$

This expression depends on the symbol rate and the frequency spacing of the channel, as well as on the fiber's dispersion (β_2) and attenuation ($L_{\text{eff,a}} = 1/2\alpha$, where α is the field attenuation parameter).

Then, assuming "standard" conditions (i.e., transmission over SMF of modern coherent optical channels), in [24, Eq. (23)] the authors provided an even simpler approximation, which was also adopted in [21]:

$$\zeta \approx \sqrt[4]{N_{\text{ch}}}\,. \tag{5}$$

The introduced error is relatively large due to the higher level of approximation. However, it proves effective while requiring only the knowledge of a single additional transmission parameter. When a more accurate estimation of ζ is required, standard NLI models (assuming that the parameters are known or can be estimated) can be used.

III. Simulation Results

A preliminary numerical analysis is performed over the simple setup in Fig. 1, in which all the fundamental steps to implement LLS-based LPM and NLI estimation are also displayed. It consists of a WDM comb of dual-polarization (DP)-64QAM channels, modulated at a symbol rate $R_s = 128$ Gbaud, and shaped by a square-root raised-cosine (SRRC) filter (roll-off $\rho = 0.1$). The simulations are carried out considering the main parameters spanning in the following ranges: number of channels $N_{\text{ch}} \in \{1, 5, 11, 21\}$, per-channel power $P_{\text{ch}} \in \{-2, \ldots, +5\}$ dBm and channel spacing $\Delta f \in \{150, 175, 200\}$ GHz. The channel of interest (COI) is the center channel. The link is composed of 10×50-km identical spans of G.652 single mode fibers (SMFs), with attenuation $\alpha_{\text{dB}} = 0.2\,\text{dB/km}$, CD coefficient $\beta_2 = -21.28\,\text{ps}^2/\text{km}$ and nonlinearity coefficient $\gamma = 1.3\ 1/\text{W/km}$. Each span is followed by an EDFA with noise figure $F = 5\,\text{dB}$ to fully compensate for the span loss. Fiber propagation is simulated using a time-domain split-step Fourier method (SSFM) and the received signal is processed by a standard DSP chain, which includes resampling at 2 sample-per-symbol, CD compensation, adaptive equalization and CPR. The output of the CPR stage is finally extracted and used as input for the LLS-based LPM and the subsequent NLI estimation algorithm. All results are compared to those obtained with a GN-model [23] running in parallel to the numerical simulations and used as a reference.

All combinations of values for N_{ch} and P_{ch} were tested, while keeping the channel spacing constant at $\Delta f = 200\,\text{GHz}$. The results are reported in Fig. 2(a), while an example of the power profiles utilized in the NLI estimation algorithm is shown in Fig.2(b), for $N_{\text{ch}} = 1$. The estimation is very accurate for the single-channel case; however, as expected, an estimation bias appears when the number of WDM channels increases, as displayed in Fig. 2(c).

IV. Experimental Validation

In this section, we evaluate the algorithm's accuracy, including XCI-based bias correction, in an experimental setup

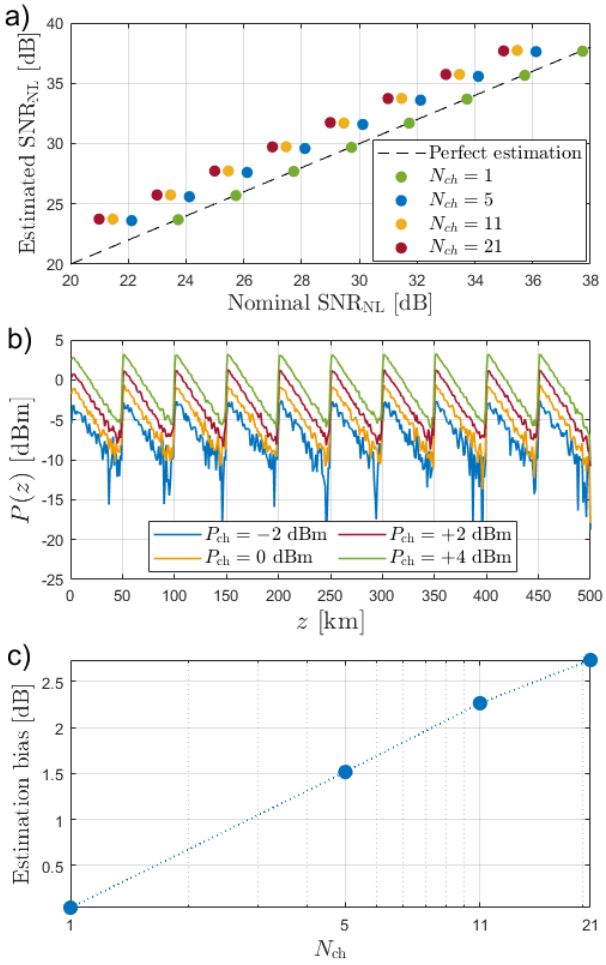

Fig. 2. a) Results of SNR_{NL} estimation using (2) with $\zeta = 1$ (circles) and the GN-model (black dashed line) over a 10×50-km SMF link at 128 GBaud per channel and $\Delta f = 200\,\text{GHz}$ for a varying number of WDM channels N_{ch}. b) Example of estimated power profiles in the single channel scenario. c) Mean estimation bias with respect to nominal SNR_{NL} computed with GN-model.

using commercial coherent transceivers. The setup is shown in Fig. 3(a) and detailed in [20]. A wide range of SNR_{NL} are explored by varying per-channel power (P_{ch}) from $0\,\text{dBm}$ to $+10\,\text{dBm}$ in $2\,\text{dB}$ steps using a VOA before the BST EDFA. For each condition, 100 profiles were estimated and used in (2) to compute the SNR_{NL}, with the final values averaged.

To validate the proposed method, the nonlinear SNR is also measured experimentally. In particular, the overall SNR is retrieved from the real-time DSP of the commercial transceiver, for each power level. The OSNR and the SNR_{TRX} are instead measured from the power spectral densities measured by the OSA and a set of back-to-back data acquisitions, respectively. Particularly, the procedure to estimate SNR_{TRX} is the one described in [25], yielding $\text{SNR}_{\text{TRX}} = 19.77\,\text{dB}$. Hence, SNR_{NL} is easily obtained from (1). The results are reported in Fig. 3(b), where the generalized SNR (GSNR) is $\text{GSNR} = (\text{SNR}^{-1} - \text{SNR}_{\text{TRX}}{}^{-1})^{-1}$. Please note that the OSNR tends to saturate around the value of $26\,\text{dB}$ at high

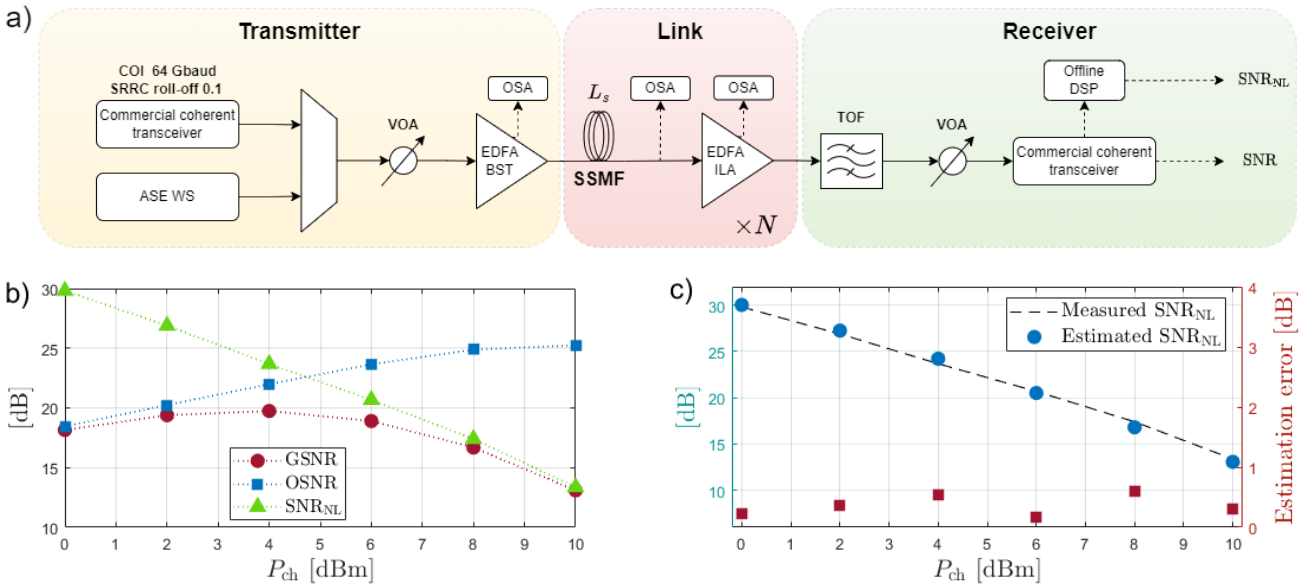

Fig. 3. a) Experimental setup. WS: wave shaper; VOA: variable optical attenuator; BST: booster; OSA: optical spectrum analyzer; ILA: in-line amplifier; TOF: tunable optical filter. b) Measured GSNR, OSNR and $\mathrm{SNR_{NL}}$ for each tested per-channel power P_{ch}. c) Comparison between measured (dashed black) and estimated (blue circles) $\mathrm{SNR_{NL}}$ with corresponding absolute estimation error (green squares).

power levels, due to the internal noise added by the transceiver, the BST and pre-amplifier EDFAs.

The measured values of $\mathrm{SNR_{NL}}$ are finally compared to those estimated by (2), as shown in Fig. 3(c). The corresponding absolute estimation error is also reported. In general, the results obtained with the proposed method are consistent with the measured values. The absolute estimation error is always below $0.6\,\mathrm{dB}$ and characterized by a root-mean-square error (RMSE) of approximately $\sim 0.4\,\mathrm{dB}$. Moreover, the simple correction factor derived in (5) proves to be effective in mitigating the estimation bias induced by XCI in the considered transmission system.

V. Impact of the Use of Hard-Decision Symbols

In this section, we investigate the performance penalty arising from using HD symbols for LLS-based LPM. To this purpose, we resort to the simple setup shown in Fig. 4(a). The transmitted WDM signal consists of $N_{\mathrm{ch}} = 11$ 150-GHz-spaced DP-16QAM channels, modulated at $R_s = 128$ Gbaud and shaped by an SRRC filter with roll-off 0.1. The per-channel power is set to $P_{\mathrm{ch}} = 5\,\mathrm{dBm}$. The link is composed by 4×50-km identical SMF spans, with attenuation $\alpha_{\mathrm{dB}} = 0.2\,\mathrm{dB/km}$, CD coefficient $\beta_2 = -21.28\,\mathrm{ps^2/km}$ and nonlinearity coefficient $\gamma = 1.3\ 1/\mathrm{W/km}$. Each span is followed by a noiseless EDFA to compensate for span loss. Fiber propagation is simulated using the SSFM. Before reception, noise loading is applied to the signal, with OSNR varied from $10\,\mathrm{dB}$ to $30\,\mathrm{dB}$, with step $1\,\mathrm{dB}$. At the receiver, the signal undergoes DSP processing, including CD compensation, adaptive equalization, CPR and decoding. The CPR output is extracted and used to perform LPM, with 2^{20} input samples and a spatial granularity equal to $\Delta z = 1\,\mathrm{km}$. A few examples of results obtained using the HD sequence for LPM are displayed in Fig. 4(b).

When error-free, the PPE aligns with the theoretical curve, but as OSNR decreases (and BER increases), an offset appears, degrading PPE accuracy. Fig. 4(c) quantifies this offset as the power difference at the beginning of the third span (i.e., $z = 100\,\mathrm{km}$) between the PPE computed with an error-free sequence and that computed with the HD sequence (which will be referred to as HD-PPE). A fitting analysis revealed a linear relation between the offset and the BER: $\psi\ [\mathrm{dB}] = k \cdot \mathrm{BER}$, with $k \simeq 100$ for the considered scenario and BER in linear units. This formula enables HD-PPE correction, improving NLI estimation accuracy.

The NLI estimation algorithm and the impact of HD-PPEs were also tested in a more realistic and challenging experimental scenario (not shown here due to space constraints) [22]. Using an error-free reference sequence, the algorithm achieved a mean absolute error of $0.5\,\mathrm{dB}$ compared to the CFM. However, with HD sequences and high BER, accuracy significantly degraded, increasing the mean absolute error to $3.5\,\mathrm{dB}$. Applying a BER-based correction to the HD-PPE offset before using (2) significantly improved accuracy, reducing the mean absolute error to $0.8\,\mathrm{dB}$. The remaining error is attributed to residual noise in the reference sequence, which affects PPEs beyond the offset correction [22].

VI. Conclusions

In this work, we described a novel method for estimating Kerr-induced NLI power in live coherent optical transmissions using only receiver DSP data. Exploiting the LLS-based LPM algorithm, it provides accurate NLI estimates and tracks WDM channel power evolution for network optimization. We also

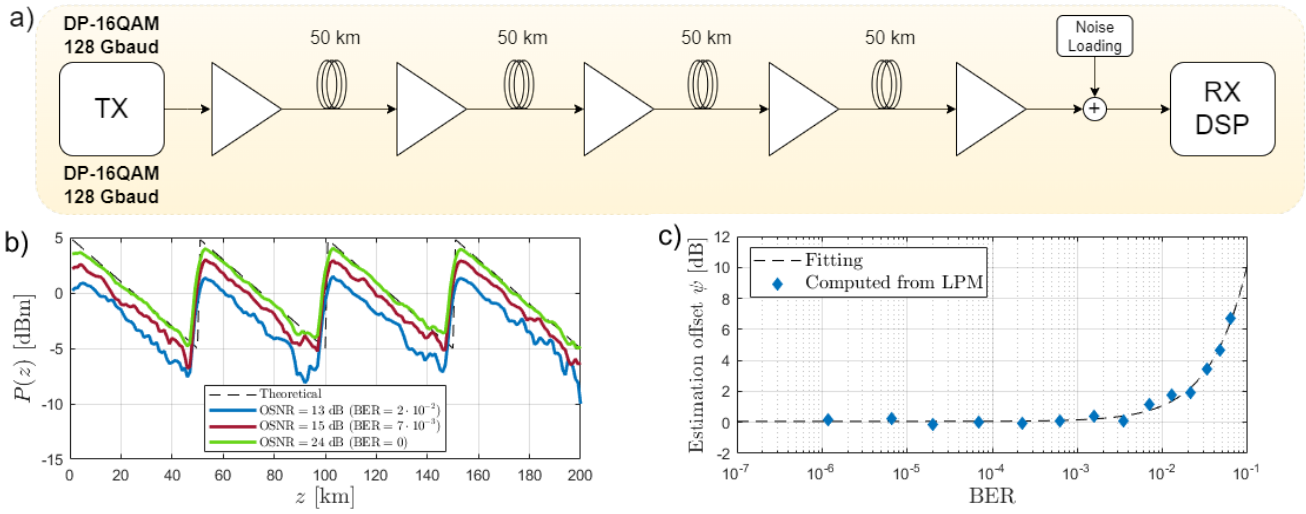

Fig. 4. a) Simulation setup. b) Power profiles computed starting from HD sequences for varying BER values. c) Estimation offset for varying BER values.

examined implementation penalties, focusing on errors from using HD reference sequences in LPM. Results showed that the offset in HD-PPEs scales with pre-FEC BER and the accuracy of the NLI estimation can be improved applying a BER-based correction.

Acknowledgments

This work was carried out in the PhotoNext Center of Politecnico di Torino and was supported by Cisco Systems through a sponsored research agreement (SRA).

References

[1] M. S. Faruk and S. J. Savory, "Measurement Informed Models and Digital Twins for Optical Fiber Communication Systems," J. Lightw. Technol., vol. 42, pp. 1016–1030, Feb.1, 2024.

[2] A. Alvarado, T. Fehenberger, Bin Chen, F. M. J. Willems, "Achievable Information Rates for Fiber Optics: Applications and Computations," J. Lightw. Technol., vol. 36, pp. 424–439, Jan.15, 2018.

[3] P. Poggiolini et al., "The GN-Model of Fiber Non-Linear Propagation and its Applications," J. Lightw. Technol., vol. 32, pp. 694–721, Feb.15, 2014.

[4] R. Dar, M. Feder, A. Mecozzi and M. Shtaif, "Pulse Collision Picture of Inter-Channel Nonlinear Interference in Fiber-Optic Communications," J. Lightw. Technol., vol. 34, pp. 593–607, 15 Jan.15, 2016.

[5] F. J. Vaquero-Caballero et al., "Machine learning based linear and nonlinear noise estimation," J. Opt. Commun. Netw., vol. 10, pp. D42–D51, Oct. 2018.

[6] A.D. Shiner, "Neural network training for OSNR estimation from prototype to product," Optical Fiber Communications Conference and Exhibition (OFC), 2022.

[7] G. Di Rosa, S. Dris, A. Richter, "Statistical quantification of nonlinear interference noise components in coherent systems," Opt. Express, vol. 28, pp. 5436–5447, Feb. 2020.

[8] F. J. Vaquero-Caballero, D. J. Ives and S. J. Savory, "Perturbation-Based Frequency Domain Linear and Nonlinear Noise Estimation," J. Lightw. Technol., vol. 40, pp. 6055–6063, Sept.15, 2022.

[9] H. J. Cho et al., "Constellation-based identification of linear and nonlinear OSNR using machine learning: a study of link-agnostic performance," Opt. Express, vol. 30, pp. 2693–2710, Jan. 2022.

[10] M. Al-Nahhal, I. Al-Nahhal, O. A. Dobre and S. K. O. Soman, "Parallel Neural Network Structures for Signal-to-Noise Ratio Estimation in Optical Fiber Communication Systems," J. Lightw. Technol., vol. 42, pp. 1941–1954, March 15, 2024.

[11] M. Boertjes, A. S. Kashi, J. C. Cartledge and W. -Y. Chan, "Machine Learning Model Training Framework for Nonlinear Signal-to-Noise Ratio Estimation in Heterogeneous Optical Networks," J. Lightw. Technol., vol. 42, pp. 4789–4799, July 15, 2024.

[12] I. Andrenacci et al., "Machine-learning-based technique to establish ASE or Kerr impairment dominance in optical transmission," J. Opt. Commun. Netw., vol. 16, pp. 481–492, Oct. 2024.

[13] T. Sasai et. al, "Recent Advances in Digital Longitudinal Monitoring of Fiber-Optic Link," Optical Fiber Communications Conference and Exhibition (OFC), 2024.

[14] T. Tanimura, S. Yoshida, K. Tajima, S. Oda and T. Hoshida, "Fiber-Longitudinal Anomaly Position Identification Over Multi-Span Transmission Link Out of Receiver-end Signals," J. Lightw. Technol, vol. 38, pp. 2726–2733, May 1, 2020.

[15] T. Sasai et al., "Digital Longitudinal Monitoring of Optical Fiber Communication Link," J. Lightw. Technol., vol. 40, pp. 2390–2408, April 15, 2022.

[16] L. Andrenacci, G. Bosco and D. Pilori, "PDL Localization and Estimation Through Linear Least Squares-Based Longitudinal Power Monitoring," IEEE Photon. Technol. Lett, vol. 35, pp. 1431–1434, Dec.15, 2023.

[17] J. Chang et al., "Demonstration of longitudinal power profile estimation using commercial transceivers and its practical consideration," 49th European Conference on Optical Communications (ECOC), 2023.

[18] T. Sasai, M. Takahashi, M. Nakamura, E. Yamazaki and Y. Kisaka, "Linear Least Squares Estimation of Fiber-Longitudinal Optical Power Profile," J. Lightw. Technol., vol. 42, pp. 1955–1965, March 15, 2023.

[19] I. Kim et al., "Nonlinear SNR Estimation based on Power Profile Estimation in Hybrid Raman-EDFA Link," Optical Fiber Communication Conference (OFC), 2024.

[20] L. Andrenacci et al., "DSP-based Nonlinear Interference Estimation using Linear Least Squares Longitudinal Power Monitoring," J. Lightw. Technol., Early Access, 2025.

[21] L. Andrenacci et al., "Nonlinear Noise Estimation using Linear Least Squares-based Longitudinal Power Monitoring," 50th European Conference on Optical Communications (ECOC), 2024.

[22] L. Andrenacci et al., "Implementation Penalties for Nonlinear Interference Estimation with Linear Least Squares Longitudinal Power Monitoring," Optical Fiber Communications Conference and Exhibition (OFC), 2025.

[23] P. Poggiolini, "The GN Model of Non-Linear Propagation in Uncompensated Coherent Optical Systems," J. Lightw. Technol., vol. 30, pp. 3857–3879, Dec.15, 2012.

[24] V. Curri et al., "Design Strategies and Merit of System Parameters for Uniform Uncompensated Links Supporting Nyquist-WDM Transmission," J. Lightw. Technol., vol. 33, pp. 3921–3932, Sept.15, 2015.

[25] Y. Jiang et al., "Experimental Test of a Closed-Form EGN Model Over C+L Bands," J. Lightw. Technol., vol. 43, pp. 439–449, Jan.15, 2025.